In vitro cytocompatibility of antibacterial silver and copper-doped bioactive glasses

Ceramics International 49 (2023) 36044–36055

Contents lists available at ScienceDirect

Ceramics International

journal homepage: www.elsevier.com/locate/ceramint

In vitro cytocompatibility of antibacterial silver and copper-doped bioactive glasses

Mari Lallukka [a], Amel Houaoui [b], Marta Miola [a], Susanna Miettinen [b,c], Jonathan Massera [b,*], Enrica Verné [a]

[a] Politecnico di Torino, Department of Applied Science and Technology, Corso Duca Degli Abruzzi 24, 10129, Turin, Italy
[b] Tampere University, Faculty of Medicine and Health Technology, Korkeakoulunkatu 3, 33720, Tampere, Finland
[c] Research, Development and Innovation Centre, Tampere University Hospital, Elämänaukio, Kuntokatu 2, 33520, Tampere, Finland

ARTICLE INFO

Handling editor: Dr P. Vincenzini

Keywords:
Bioactive glass
Silver
Copper
Cytocompatibility
Human adipose stem cells

ABSTRACT

Fighting the formation of bacterial biofilm and simultaneously providing a bioactive environment for bone regeneration during the treatment of orthopedic infections is one of the greatest challenges in surgery. Moreover, the major global threat of rapidly increasing antimicrobial resistance calls for non-antibiotic alternatives. Bioactive glasses doped with antibacterial metal ions silver (Ag), or copper (Cu), offer a potential solution. However, an added challenge is the cytocompatibility of these antimicrobial biomaterials, which could be compromised due to the possible cytotoxic effect of the dopants.

This work evaluates the cytocompatibility of two bioactive glasses, SBA2 and SBA3, either doped with Ag- (Ag-SBA2) or Cu-ions (Cu-SBA3) via ion-exchange process. The viability, proliferation, and morphology of human adipose stem cells (hASCs) were evaluated using different culture conditions: i) direct culture on glass discs, with and without pre-incubation, and ii) in medium containing glass dissolution byproducts. The release kinetics of the doped ions was evaluated in α-MEM and during cell culture. Moreover, the effect of protein adsorption on the cell response was studied by introducing a layer of fibronectin on the glass discs before direct culture with hASCs.

Ag-SBA2 and Cu-SBA3 both initially inhibited the hASC viability in direct cell culture. However, cells remain viable with healthy morphology when cultured directly on pre-treated discs, or indirectly with the glass dissolution byproducts. This suggests that the cytotoxicity effect seems to arise from the contact toxicity between the cells and the material surface. Fibronectin adsorption significantly improved the cytocompatibility of Ag-SBA2, while Cu-SBA3 requires further optimization. To conclude, Ag-SBA2, through its contact toxicity, has the potential for treating early infection, without compromising long-term cytocompatibility and bioactivity. However, further optimization of the Cu-SBA3 glass is needed due to its cytotoxicity towards hASCs.

1. Introduction

The number of bone defects, due to the aging population, will be more evident in the future [1]. Despite the majority of performed surgeries being successful, the adhesion of several micro-organisms, such as bacteria, viruses, or fungi, to the implantation site is still a major cause of implant failure [2]. Unfortunately, the rapid increase in orthopedic surgeries combined with the challenging bacterial resistance phenomenon, and reduced availability of new antibiotics, leads to a great demand for non-antibiotic alternatives outside conventional methods to treat orthopedic infections [3].

Bacterial infections are increasingly difficult to treat, and therefore, they remain a major threat globally in healthcare [4]. In general, bone infections are treated with systemic administration of antibiotics [5]. One factor contributing to the failure of conventional antibiotic treatments and the development of highly resistant bacteria is the formation of biofilm. Biofilm can be defined as an aggregation of bacteria embedded within their self-produced biopolymeric structure. Biofilm prevents antibiotics penetration but also contributes to bacterial survival due to its nutrient and waste transport channels [6]. Orthopedic infections are mainly caused by gram-positive staphylococci, such as *Staphylococcus aureus*, and especially its methicillin-resistant version (MRSA) [7].

In the context of musculoskeletal tissue regeneration, bioactive

* Corresponding author.
E-mail address: Jonathan.massera@tuni.fi (J. Massera).

https://doi.org/10.1016/j.ceramint.2023.08.284
Received 28 April 2023; Received in revised form 21 August 2023; Accepted 24 August 2023
Available online 31 August 2023

glasses (BAGs) and glass-ceramics are excellent options owing to their inherent ability to bond with living bone by initial glass dissolution in a fluid environment and the following precipitation of hydroxyapatite on their surfaces [8]. Moreover, bioactive glasses are osteostimulative, indicating their stimulation of bone growth away from the bone-implant interface by recruiting and stimulating cells to form new bone [9].

Currently, several different antibiotic-free approaches are being studied and developed. They can work either to passively prevent bacteria attachment (anti-fouling) or actively directly kill them (bactericidal) [6]. Biocide metallic ions such as silver (Ag^{+}), copper (Cu^{2+}), zinc (Zn^{2+}), gallium (Ga^{3+}), and cerium (Ce^{4+}) -ions are known for their inherent antimicrobial properties [10–15]. Moreover, the addition of metallic ions could also favor bone regeneration and osteogenesis [2].

Biocide ions can be used as dopants in bioactive glasses. In general, metallic ions kill bacteria by either producing reactive oxygen species (ROS), or by interacting with the bacterial cell membrane. These actions can ultimately lead to compromised electron transport destroying bacterial DNA, or to bonding of the metallic ions to functional groups of the bacteria membrane altering cell metabolism and activity. These mechanisms can also work in synergy when two or more ions are applied simultaneously [16].

Both silver (Ag^{+}) and copper ions (Cu^{2+}) are well known for their broad-spectrum antibacterial performance and low bacterial resistance. Firstly, Ag-ions can disrupt bacterial cell membranes by binding to thiol groups in proteins and DNA in the cytoplasm environment. However, some concerns are raised due to its toxicity, especially in the case of silver nanoparticles (AgNPs) [17]. For instance, Xie and co-workers found AgNPs to compromise the viability of osteoblast-like MG-63 cells when exposed to AgNPs, with the effect continuing even after the removal of AgNPs from the culture medium [18]. Copper, however, is known to be less cytotoxic to human cells, and it also plays an important role in the metabolism of bone regeneration and angiogenesis [19]. In general, for both ions, the antibacterial performance is known to be dose-dependent, with bacteria commonly being more sensitive toward silver ions [20].

Metallic ions are most often incorporated in the glass during the glass melting or sol-gel process. For instance, both Cu- and Ag-doped silicate sol-gel BAGs were synthesized by Palza et al., also demonstrating their antibacterial activity against ampicillin-resistant *Escherichia coli*, and *Streptococcus mutans* [21]. Another study comparing Ag- and Cu-doped sol-gel glass found that Cu-doped glass provided a more long-term antibacterial effect due to the more prolonged release of ions [22]. In addition to sol-gel glasses, silver has also been incorporated for example to borate glasses by a melt-quenching technique by replacing Na_2O with varying amounts of Ag_2O [23]. The Ag-doped borate glass exhibited good bioactivity and biocompatibility towards MC3T3-E1 cells with Ag_2O concentration being less than 0.75 mol%, and bactericidal effect against *Escherichia coli,* and bacteriostatic effect against *Staphylococcus aureus*.

One interesting option to introduce metallic ions to glass without modifying its bulk properties is surface doping via the ion-exchange method in an aqueous solution. In this process the monovalent ions from the surface of the glass are being released and replaced by the ions of interest present in the ion exchange aqueous solution, such as silver or copper ions. This method is beneficial due to its simplicity and possibility to introduce ions of interest on the surface without unwanted crystallization phenomena. The ion-exchange process for SBA2 to obtain Ag-doped glass Ag-SBA2 [24], and for SBA3 to obtain Cu-doped glass Cu-SBA3 has been previously optimized by Miola et al. [25,26]. The glass Ag-SBA2, also in focus for this work, has been previously studied in a co-culture with human osteoblast progenitor cells (hFOBs) and a pathogenic drug-resistant (Methicillin-Oxacillin) certified strain of *Staphylococcus aureus*, evidenced its antibacterial performance and cytocompatibility [27]. In addition, initial evaluation of the antibacterial performance of Cu-SBA3 powder has performed with satisfactory results against *S. aureus* [25].

This study aims to gain a deeper understanding of the cytocompatibility of Ag- and Cu-doped multifunctional bioactive glass surfaces obtained by the ion-exchange process by assessing human mesenchymal stem cells' behavior in contact with these surfaces, comparing different test methods. Firstly, the viability and proliferation of hASCs are evaluated in direct culture on glass discs and indirect culture with the glasses' dissolution products. In addition, the release kinetics of doped antibacterial ions Ag^{+} and Cu^{2+} are studied in culture medium alone and during cell culture. Finally, the impact of fibronectin adsorption and addition of pre-incubation step on hASCs viability in direct culture is determined.

2. Materials and methods

2.1. Synthesis of the glasses and ion-exchange process

Two different silica-based bioactive glasses, SBA2 [24], and SBA3 [25] (that belong to SiO_2–Na_2O–CaO–P_2O_5–B_2O_3–Al_2O_3 system) were prepared in the bar form using the melt and quenching technique. The oxide compositions are summarized in Table 1.

Shortly, the glass precursors were mixed and then melted in a platinum crucible at 1450 °C for 1 h, poured into a pre-heated cylindrical brass mold (Ø = 10 mm) to obtain bars, and then annealed at 500 °C for 13 h. All the cylindrical glass bars were cut into 2 mm thick discs (Buehler IsoMet High Speed Pro), which were then polished (Struers LaboPol-2) with SiC abrasive papers ranging from 320 to 1200 grid to level the disc surfaces.

Then, the sample discs went through a previously optimized and published ion-exchange process in an aqueous solution in order to incorporate therapeutic ions on the samples' surface [24,25]. As shown in these previous works, the ion-exchange solution concentrations were chosen based on their ability to cause an antibacterial effect without modifying the phase composition of the glass with nucleation of unwanted crystalline peaks of silver/copper salts. Ag-SBA2 and Cu-SBA3 were produced by soaking the discs in a 0.03 M AgNO3 and 0.001 M copper acetate (Cu(CH3COO)2·H2O) solution, respectively, for 1 h at 37 °C. After the process, the samples were rinsed with bi-distilled water and dried at room temperature overnight.

Before use in cell culture experiments, the sample discs were heat sterilized for 3 h at 100 °C and stored at room temperature until use.

2.2. Glasses immersion and ion release analysis

The samples were immersed in 1 mL of α-Minimum Essential Medium pure culture medium (α-MEM, Gibco, Thermo Fisher Scientific, without serum and antibiotics) for 7 days. To analyze the ion release, the glass dissolution products were collected and analyzed using inductively coupled plasma-optical emission spectrometry (ICP-OES; Agilent 5100 ICP-OES). The analyzed elements included Ag (λ = 328.068 nm), and Cu (λ = 223.009 nm). The measurements were conducted in three separate samples at each time point for each composition and the results are presented as mean ± standard deviation.

The wettability of the doped glasses compared to the undoped ones was assessed by static contact angle measurement by the sessile drop method (Krüss DSA 100, KRÜSS GmbH). Ultrapure water was used as a wetting fluid. A drop of water (5 μL) was deposited on the surface with a pipette and the contact angles were measured through the instrument software (DSA-100, Dropshape Analysis, KRÜSS GmbH). In addition, before and after three days of soaking in the α-MEM pure culture

Table 1
Nominal compositions of SBA2 and SBA3 melt-derived glasses.

mol-%	SiO_2	Na_2O	CaO	P_2O_5	B_2O_3	Al_2O_3
SBA2	48.00	18.00	30.00	3.00	0.43	0.57
SBA3	48.00	26.00	22.00	3.00	0.43	0.57

medium, the sample surfaces were analyzed by energy-dispersive X-ray spectroscopy (0 day results: JCM-6000 Plus Benchtop SEM, Jeol, equipped with EDS; 3 day results: EDS, Oxford Instruments X-MaxN 80) to study the effect of soaking to the ion-exchanged surface layer of Ag- or Cu-ions.

2.3. Cell analysis

2.3.1. Ethics statement

Human adipose stem cells (hASCs) were isolated from a subcutaneous abdominal tissue sample obtained from a female donor (age 49 years, BMI 21.4) at the Tampere University Hospital Department of Plastic Surgery with the donor's written informed consent and processed under ethical approval of the Ethics Committee of the Expert Responsibility area of Tampere University Hospital (R15161).

2.3.2. Adipose stem cell isolation and expansion

The cells were isolated as described previously [28]. The mesenchymal origin of hASCs was confirmed by surface marker expression analysis with flow cytometry [29] and the ability of adipogenic and osteogenic differentiation [30] by Oil Red O and Alizarin Red staining, respectively. The cells were characterized as MSCs due to positive expression of CD73 (97%), CD90 (99%), and CD105 (99%), and low or negative expression of CD14 (1%), CD19 (0.6%), CD45 (2.6%), CD34 (8%) and HLA-DR (0.9%) [31,32] as well as accumulation of lipid droplets by Oil Red O and mineralized matrix deposition by Alizarin Red staining.

The isolated hASCs were maintained in T-75 polystyrene flasks (BioLite, Thermo Fisher Scientific) in α-Minimum Essential Medium (α-MEM, Gibco, Thermo Fisher Scientific) supplemented with 5% Human Serum (HS, Serana Europe GmbH), and 1% antibiotics (100 U/ml penicillin and 0.1 mg/ml streptomycin; Gibco, Thermo Fisher Scientific). The cells were cultured in an atmosphere of 5% CO_2 at 37 °C. When 80–100% confluence was reached, hASCs were cryo-preserved in gas-phase nitrogen in a freezing solution (HS supplemented with 10% dimethyl sulfoxide; DMSO Hybri-Max®, Sigma–Aldrich) and thawed when needed for the experiments.

For all experiments, confluent cells between passages 3–5 were used. All the experiments were conducted in 48 well plates (Nunc, Roskilde, Denmark), with α-MEM culture medium supplemented with 5% HS and 1% antibiotics (basic culture medium). A cell amount of 10 000 cells/well was used. Cells controls were seeded in tissue culture polystyrene (TCPS) 48 well plate (Nunc).

2.3.3. Direct and indirect cell culture

Experiments done in direct culture: Glass discs of 1 cm in diameter were placed in 48 well plate and hASCs were seeded on the discs (10 000 cells/well). The culture medium was changed every 72 h and the experiment was carried out for up to 7 days.

Experiments done in indirect culture: Glass discs were immersed in 1 mL of basic culture medium for 24 h at 37 °C. In parallel, the hASCs were seeded in 48 well plates (10 000 cells/well), in a basic culture medium. After one day of culture, the basic culture medium was replaced by the conditioned medium coming from the glass discs' incubation (Fig. 1). A fresh basic culture medium was added to the glass discs and every 48 h, the dissolution products were used as a culture medium for the cells

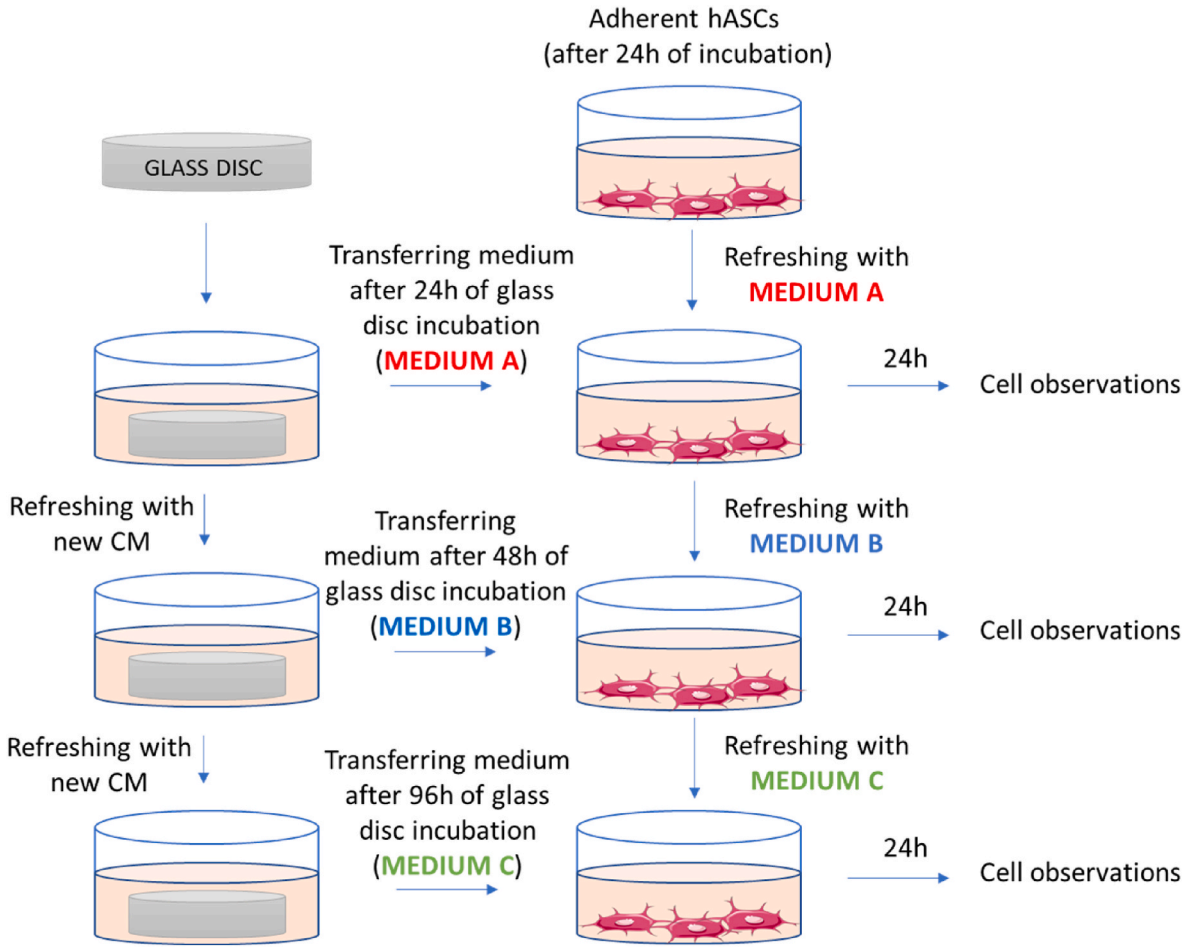

Fig. 1. Protocol of indirect culture. CM = basic culture medium (alpha-MEM, 5% HS, 1% P/S), glass disc incubation medium (Medium A, B, C) includes glass disc dissolution products (conditioned medium).

(conditioned medium), to investigate the effect of the ion release during the time on cells without having any contact between the cells and the glass discs. Finally, this test was done for up to 7 days of culture. Both Ag-SBA2 and Cu-SBA3 were tested, and cells cultured in TCPS 48 well plate only with basic culture medium were used as a control. One day after each time the dissolution products were put in contact with cells, the cells were observed by imaging with the microscope Nikon Eclipse Ts2-FL combined with a camera DFK 33UX174 from The Imaging Source.

2.3.4. Fibronectin coating

Fibronectin coating on the glass discs was tested to see if it can improve cell attachment and viability. The surfaces of the discs were Fibronectin-coated before cell culture. A solution of Fibronectin was prepared in PBS (69 mM NaCl, 1.3 mM KCl, 19.6 mM $Na_2HPO_4{\cdot}2H_2O$, 3.3 mM KH_2PO_4, pH 7.4) at a concentration of 15 μg/mL. The whole surface of each sample (a drop of 200 μL) was covered with Fibronectin solution for 1 h at 37 °C.

Before cell culture, the grafting of Fibronectin on the glasses was ensured by using fluorescently labeled fibronectin (Alexa Fluor 488 NHS Ester, AAT Bioquest, Inc., CA). The labeling was done by fluorescent tag, and it was performed according to instructions of the manufacturer and confirmed by laser scanning confocal microscope observations (Zeiss LSM 800).

2.3.5. Pre-incubation step

A pre-incubation step was tested for cell culture. The samples were pre-incubated for 24 h in 1 mL of basic culture medium before cell culture to investigate if cell viability could be improved.

The different methods used to investigate the behavior of hASCs with the glass discs are summarized in Fig. 2.

2.3.6. Cell viability and proliferation

Cell viability on BAG discs after 1, 3, and 7 days were analyzed with Live/Dead staining (Invitrogen, Thermo Fisher Scientific). Briefly, cells were incubated in a working solution containing 0.25 μM EthD-1 and 0.5 μM Calcein-AM for 40 min at room temperature. This was followed by immediate imaging (IX51, Olympus, Tokyo, Japan, equipped with a fluorescence unit and Hamamatsu Orca Flash 4.0LT + sCMOS camera).

Cell proliferation on BAG discs was assessed after 1, 3, and 7 days of culture using CyQUANT Cell Proliferation Assay (Invitrogen, Thermo Fisher Scientific), according to the manufacturer's protocol. Shortly, samples were lysed in 0.1% TritonX-100 lysis buffer (Sigma-Aldrich) and stored at −80°. Three parallel 20 μl replicates of each lysate were pipetted to a 96-well plate (Nunc) and mixed with 180 μl working solution containing CyQUANT GR dye and cell lysis buffer. The fluorescence at 480/520 nm was measured using a plate reader (Victor 1420 Multilabel counter, Wallac, Turku, Finland).

2.3.7. Cytochemical staining

The morphology of the cells seeded on pre-incubated samples was observed after 1, 7, and 14 days of culture. At each time point, the cells were fixed with 4% (w/v) para-formaldehyde solution for 15 min, then permeabilized with 0.1% (v/v) Triton X-100 for 10 min. Non-specific binding sites were blocked by incubating the samples in PBS with 1% Bovine Serum Albumin (BSA) for 1 h. The actin cytoskeleton was stained with 1:500 FITC-labeled phalloidin and the nuclei with 1:1000 4',6-Diamidino-2-phenylindole dihydrochloride (DAPI) in PBS-BSA 0.5% for 1 h. The incubation of antibodies was performed in a moist chamber covering them from light. After incubation, the samples were washed with PBS-BSA 0.5% and pure water and observed using a fluorescence microscope (IX51, Olympus, Tokyo, Japan, equipped with a fluorescence unit and a camera DP30BW, Olympus).

2.3.8. Culture medium analysis

The ion release of the samples in the culture medium during the pre-incubation step and/or the cell culture were analyzed as presented above (2.2) by ICP-OES. To analyze the ion release, the glass dissolution products during pre-incubation and cell culture were collected and the elements Ag (λ = 328.068 nm), B (λ = 208.956 nm), Ca (λ = 396.847 nm), Cu (λ = 223.009 nm), Na (λ = 589.592 nm), P (λ = 213.618 nm), Si (λ = 251.611 nm) were analyzed. The measurements were conducted in three separate samples at each time point for each composition and the results are presented as mean ± standard deviation.

2.3.9. Statistical analysis

Data were analyzed using GraphPad Prism Software. Statistical significance between groups is assessed by one-way analysis of variance

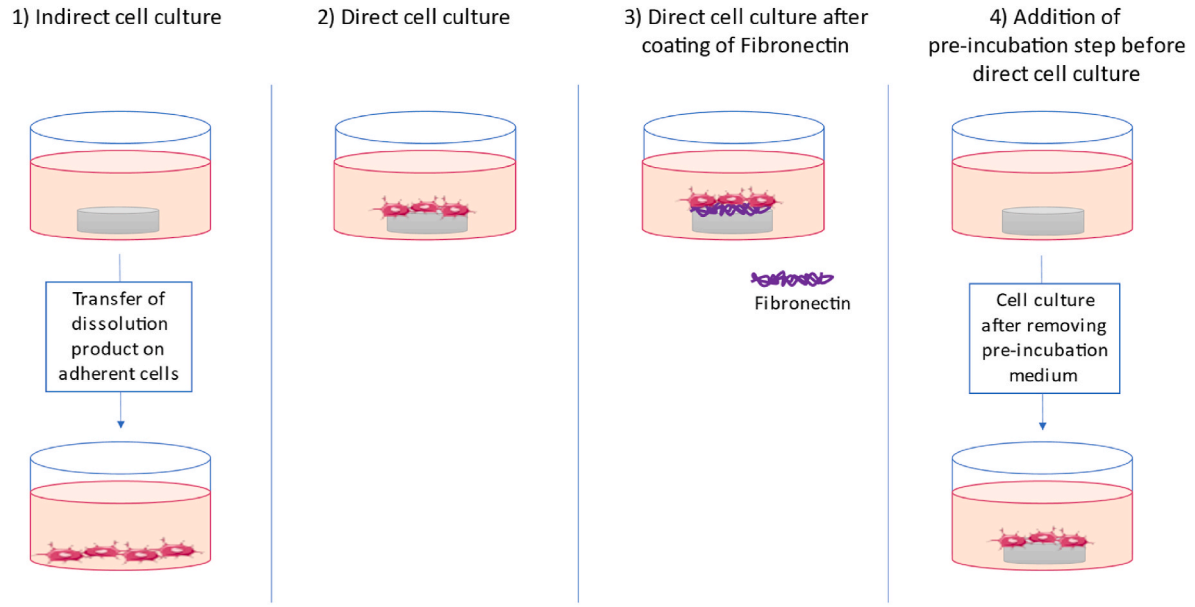

Fig. 2. Methods used to study the cytocompatibility of the ion-doped specimens. 1) Indirect cell culture with adherent cells in contact with specimen dissolution products as presented in Figs. 1 and 2) Direct cell culture on top of the specimen discs, 3) Direct cell culture on top of fibronectin-coated specimen discs, and 4) Direct cell culture on top of pre-incubated specimen discs.

(ANOVA). Experimental results are expressed as means ± standard deviation. Statistical significance is taken for values of $p < 0.05$.

3. Results and discussion

3.1. Doped glasses characterization

Some data from physicochemical surface characterization of Ag-SBA2 and Cu-SBA3 were previously reported by the authors. To summarize, the surface composition of Ag-SBA2 has been analyzed with XPS and EDS, showing the uniform distribution of Ag-ions on the glass surface replacing the Na-ions. In addition, the transmission electron microscopy (TEM-EDS) on the glass cross-sections showed the presence of silver as a very thin layer on the glass surface [24,27]. For Cu-SBA3 the physicochemical characterization has been performed to the glass in a powder form, as reported by the authors [25]. In the study, a layer of copper was found on a glass surface as ionic Cu(II) replacing Ca- and Na-ions, as evidenced by EDS and XPS. Further physical characterization of the Cu-SBA3 is planned for the future. In addition, both doped glasses have been shown to have antibacterial properties against S. aureus, as reported by the authors [25,27].

Due to the expected lower toxicity of copper ions compared to silver ions [19], the comparison between Ag-SBA2 and Cu-SBA3 cytocompatibility is of interest in the current study. In the present research the surface characterization was performed through wettability analysis by static contact angle measurement, followed by the EDS analysis of the glass surfaces before and after soaking in cell culture medium, and the quantification of released Ag/Cu-ions by ICP-OES to further understand the cytocompatibility results obtained in the same research. The results from EDS, ICP-OES, and contact angle measurement are reported in Figs. 3–5.

Soaking of doped glasses, Ag-SBA2 and Cu-SBA3, in pure α-MEM culture medium without added serum and antibiotics for up to 7 days was performed to evaluate the kinetics of silver and copper release in conditions close to cell culture. The concentrations of released Ag (A) and Cu (B) in pure α-MEM are reported in Fig. 3.

According to Fig. 3A, both surface-doped glasses release most of the doped ionic Ag/Cu during the first day of soaking. In the case of Ag-SBA2, the release of Ag from the surface occurs in a slightly more controlled manner over multiple days, the maximum value being about 7400 μg/L after seven days of soaking. However, in terms of Cu-SBA3, the maximum value of released Cu ions (about 10 000 μg/L) is reached already on the first day. For both glasses, the standard deviation for the ion release was found to be high, which raises questions about whether the amount of doped ions varies between ion-exchanged samples. In addition, some concerns about the accuracy of the measured amount of silver release by the ICP-OES technique can be raised, since it could be affected by the high affinition of silver with proteins present in serum [33]. In this measurement, the ion release was performed only in α-MEM without added serum, which minimizes the issue.

EDS results (Fig. 4) were found to be well in agreement with the ICP-OES results. After three days of soaking in α-MEM, a very low amount (<1 wt-%) of Cu-ions seems to be present on the Cu-SBA3 sample surfaces, compared to the initial amount of around 16 wt-%. This suggests that the Cu-ion layer is completely released in only a couple of days of soaking. In the case of Ag-SBA2, it seems that after soaking for 3 days, there is still a remaining layer of silver ions on the samples, since the EDS results both before and 3 days after soaking show around 1 wt-% of silver. The remaining silver on the soaked discs can also be seen with naked eye as a brown color on the disc surface. This is also shown in the ICP-OES analysis with more controlled silver ion release over multiple days. However, it should be noted that the penetration depth of EDS analysis is known to be higher than one micron, which might undermine the usability of this method for evaluating thin surface layers [34]. The thickness of the Ag-ion layer of Ag-SBA2 has been previously estimated to be a few nanometers through transmission electron microscopy (TEM) by the authors [27], and therefore, other methods, such as X-ray photoelectron spectroscopy (XPS) or secondary ion mass spectroscopy (SIMS) with lower penetration depth could further clarify the chemical composition of the ion-exchanged surfaces [35]. In the case of Ag-SBA2 the XPS results are already reported previously by the authors [27], even more confirming the presence of ionic silver as an outermost layer on the glass surface.

ICP-OES and EDS results show an initial burst release of the doped ions from the glass surface. This release could be detrimental to cell viability. To investigate that, the behavior of hASCs in presence of these glasses has been studied with different methods. Also, the ion release from these glasses during cell culture experiments has been investigated.

In addition, the effect of ion exchange to the surface wettability (hydrophobicity/hydrophilicity) of the glasses was investigated. In Fig. 5 the contact angles of the undoped and Ag/Cu-doped glasses are reported.

In general, both bioactive glass composition SBA2 and SBA3 are found to be hydrophilic with a contact angle around 20–30°. The ion-exchange process is seen to increase the contact angle in both cases of Ag- and Cu-doping. Especially the Cu-doping by ion exchange is seen to increase the contact angle up to 50°. According to the literature cells are known to better attach to hydrophilic surfaces [36]. Ensuring the cell attachment is essential for the further cell spreading and proliferation, and therefore the survival of anchorage-dependent cells, such as mesenchymal stem cells also of interest of the present research.

3.2. Cellular characterization of the glasses

3.2.1. Indirect cell culture

First, to study the cytocompatibility of the different glasses doped with Ag- and Cu-ions, the effect of the extracts coming from the glasses immersed in a culture medium was investigated by doing an indirect

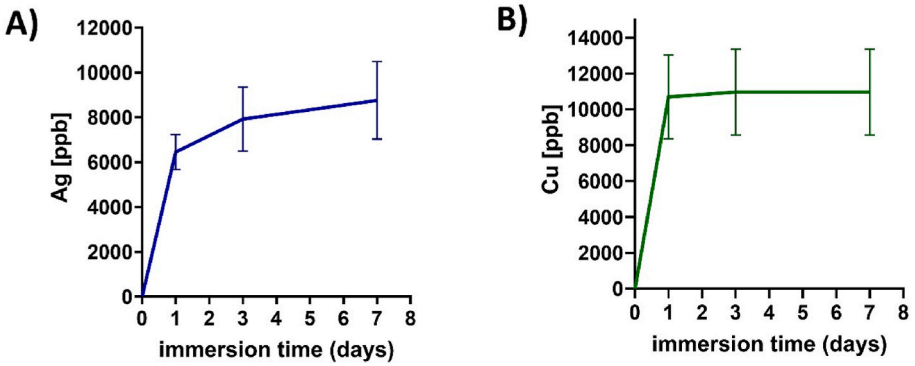

Fig. 3. Release of ion-exchanged Ag-ions from Ag-SBA2 (A) and Cu-ions from Cu-SBA3 (B) up to 7 days in pure α-MEM culture medium analyzed by ICP-OES.

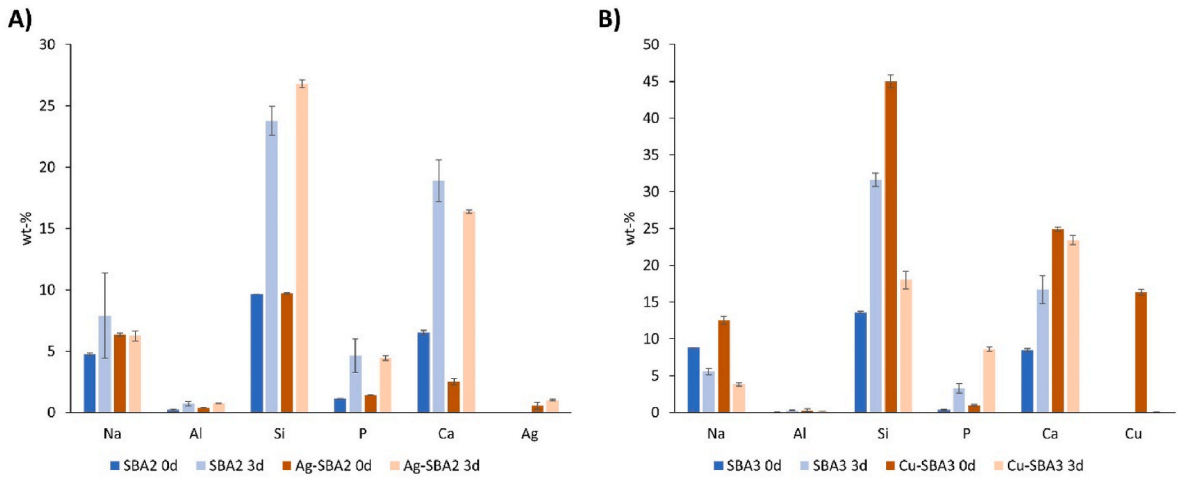

Fig. 4. EDS results in weight percentages of the surfaces of A) SBA2 and Ag-SBA2 before (0d) and after [3d] soaking in α-MEM, and B) SBA3 and Cu-SBA3 before (0d) and after [3d] soaking in α-MEM.

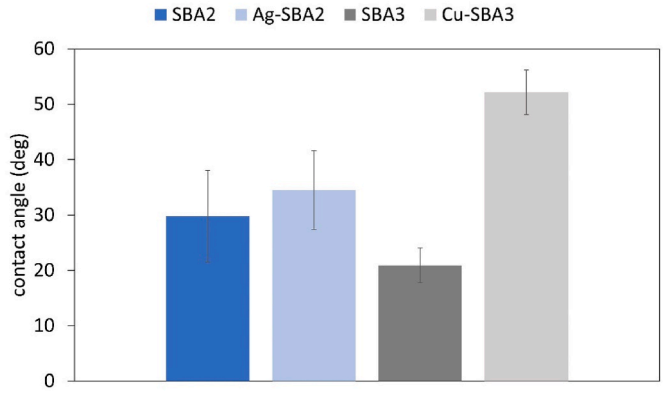

Fig. 5. Wettability of the Ag-SBA2 and Cu-SBA3 compared to their undoped controls SBA2 and SBA3, respectively.

cytotoxicity test. Adherent cells were exposed to the extracts in the conditioned medium for up to 7 days. Fig. 6 shows the images of the cells cultured in the conditioned medium for 1 day, 3 days, and 7 days (on the left) and Ag- and Cu-ion concentrations in the conditioned medium used for the cell culture (on the right). For the dissolution products of both doped glasses, no inhibitory effect on hASCs spreading and growing was detected at any time point, when compared to the control images (cell grown on TCPS with normal medium without glass dissolution products). In addition, no changes in cell morphology were detected. These results show that the glass extracts containing the released ions are probably not toxic to the cells.

The result for Ag-SBA2 is in line with previously published cytocompatibility analysis with human progenitor osteoblasts (hFOBs) [27], where Ag-SBA2 samples were found cytocompatible. In the case of Cu-SBA3, no previous cell studies have been published. In the literature, there are different concentrations of Cu-ions stated to be toxic for hASCs. For example, Thyparambil et al. found a decrease in hASCs viability with Cu-doped (0.4 wt-%) bioactive glass 13–93B [37], while Mishra et al. reported cytotoxicity of undiluted Cu-doped borophosphate glass

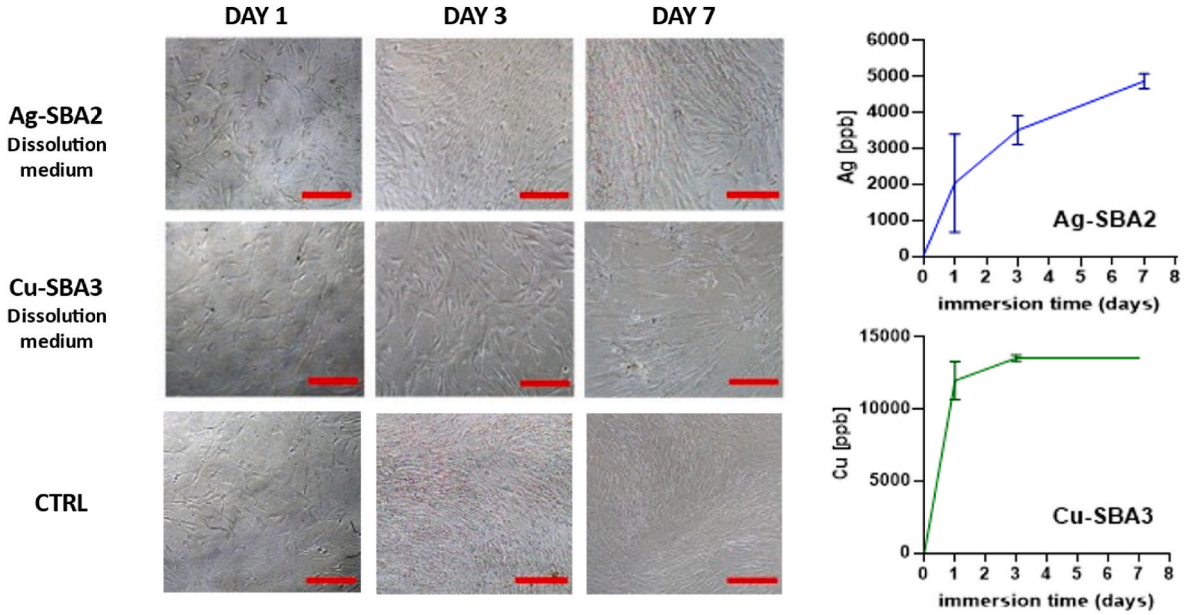

Fig. 6. Light microscopy images of hASCs cultured with the glass dissolution products (left) and graphs showing the corresponding released concentration of doped ions (Ag or Cu) by ICP-OES analysis (right). Scale bars 200 μm.

extract, Cu ion concentration being around 2 ppm, towards hASCs [38]. Dose-dependent toxicity of Cu has also been evidenced in mouse fibroblasts, where the median lethal dose of Cu-ions was found to be around 46 ppm [39]. The values seem to vary depending on the sample, culturing conditions and used cell line, and therefore, it is challenging to compare with concentrations detected in this work. In our indirect culture experiment, the concentration of Cu-ions in the medium does not appear to be cytotoxic to the cells.

3.2.2. *Direct 2D cell culture and effect of fibronectin coating*

After confirming the cytocompatibility of the glass extracts, hASCs viability was studied upon direct culture on glass discs by live/dead staining after 1, 3, and 7 days of culture.

As seen in Fig. 7, the undoped glasses (SBA2 and SBA3) supported the cell viability, similarly to the positive control, thus demonstrating that the glass composition is suitable for cell culture. Ag-SBA2 seems to inhibit cell viability after 1 day of culture, however, the cell number appears to increase slightly after 3 days. Therefore, one can hypothesize that the fast release of Ag-ions over the first day of culture is toxic to cells, but the toxicity decreases for a longer immersion time, with the changes of the medium, showing the cells trying to recover. In the case of the Cu-SBA3, it appears to be highly toxic in 1 day, killing all the cells. No living cells can be seen on day 1 and therefore they cannot recover later. This agrees with the high Cu-ion release occurring on day 1 evidenced by ICP-OES analysis (Fig. 3). However, as shown in the indirect cell culture (Fig. 6), the cytotoxicity of doped glasses does not seem to arise from the concentration of the released ions in the medium, but rather from the fast release and the direct contact of the hASCs to the sample surface. This type of contact-killing phenomenon could arise due to factors such as local burst release of ions, redox or catalytic activities of the ions, or the formation of reactive oxygen species [40,41].

To promote cell adhesion, viability, and proliferation [42], while maintaining the release of ions from the glasses, each material was coated with fibronectin, as shown in Fig. 8.

Before cell culture, all samples were coated with fluorescently labeled fibronectin and imaged by confocal fluorescence microscopy to confirm protein adsorption. The green fluorescence in the images can be assigned to the fluorescently labeled fibronectin because no autofluorescence was observed on any of the sample surfaces. As reported previously by Azizi et al. [43], adsorption of fibronectin on the silicate-based bioactive glass can promote cell adhesion and spreading. The confocal images (Fig. 6) confirm that the fibronectin was adsorbed and homogeneously covering the sample discs for each condition, which is expected to improve the cell adhesion.

After checking the uniform adsorption of fibronectin on the glass discs, cell culture was performed on the materials with the adsorbed fibronectin, and the live/dead images are presented in Fig. 9.

The fibronectin-coating can be seen to enhance hASC viability and proliferation, especially in the case of Ag-SBA2. More viable cells are observed at all time points compared to Ag-SBA2 without added fibronectin (Fig. 7). In the case of Cu-SBA3, fibronectin adsorption does not seem to improve cell viability, as seen in Fig. 9 with red cells indicating cell death. However, the fibronectin may delay the release of Cu-ions, as some cells appear to be alive on day 1, but their death is evident only after 3 days of culture.

This observation is also supported by the quantitative CyQUANT cell proliferation assay (Fig. 10). Without fibronectin coating (Fig. 10A), the cell number of hASCs is significantly decreased with the doped Ag and Cu glasses compared to SBA2 and SBA3 respectively. Fig. 10B shows that even with the fibronectin coating, the same significant decrease is still observed. However, when the doped glasses are compared with and without fibronectin (Fig. 10C), it is observed that the fibronectin allows a significantly higher cell proliferation on day 1 for Cu-SBA3 glass and days 1 and 7 for Ag-SBA2. Differences in values between the different conditions on day 1 could be due to differences in viability, different attachment efficiencies as well as differences in proliferation rates. However, these results show that even if the fibronectin allows an improvement of cell proliferation on the doped glasses, it is still not enough to reach the ability to support the proliferation of the SBA2 and SBA3 glasses.

To verify that the coating of adsorbed fibronectin does not prevent the release of Ag/Cu-ions from the glass surfaces, ICP-OES analysis was performed for the cell culture medium from both the direct culture with and without fibronectin. The release kinetics of these ions in the cell

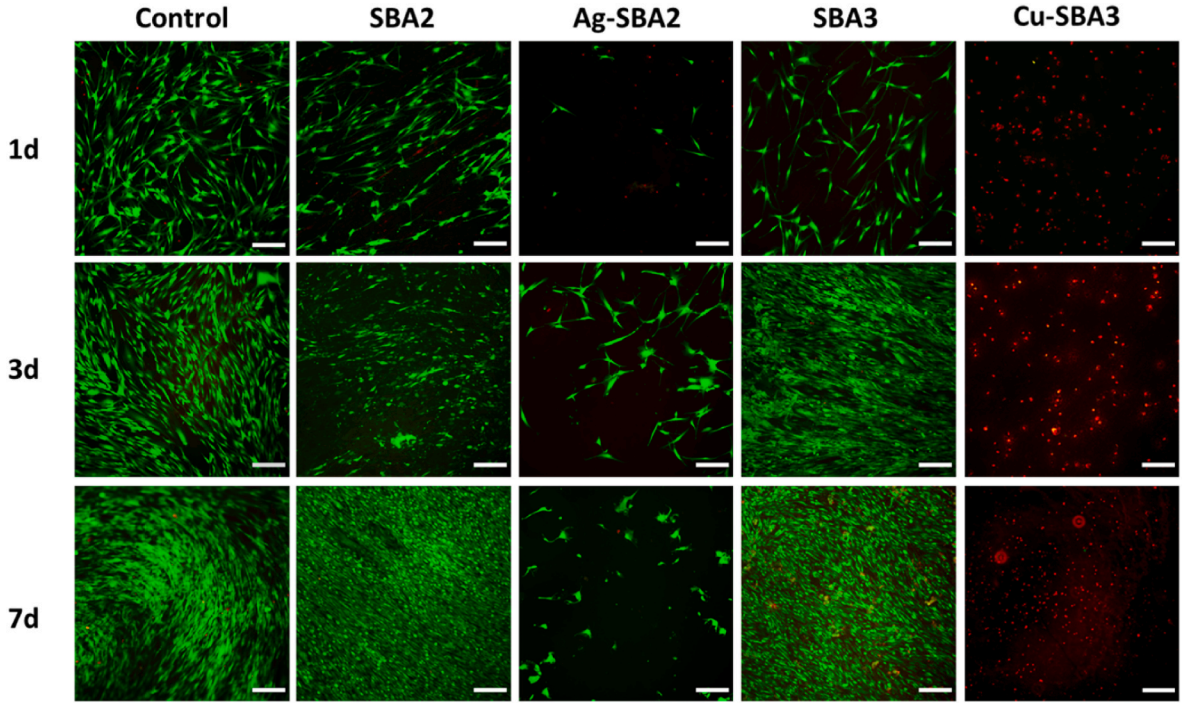

Fig. 7. Cell viability on bioactive glass discs at 1, 3, and 7d. Viability was analyzed with Live/dead staining. Scale bars 200 μm.

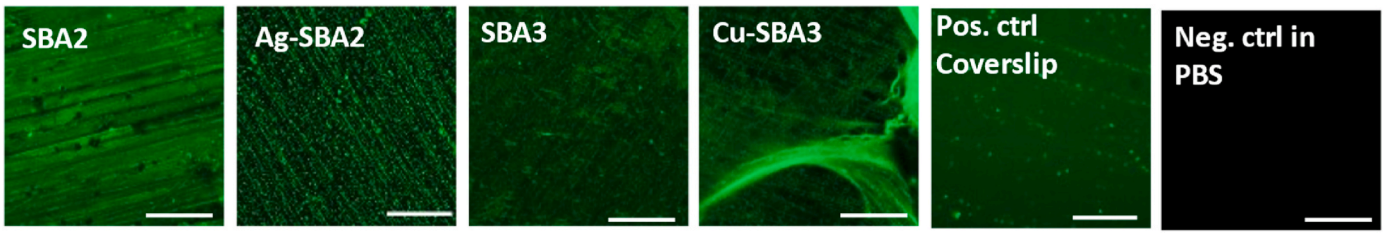

Fig. 8. Confocal microscopy images of the glasses surface with adsorbed 488-Alexa labeled fluorescent fibronectin. Scale bars 30 μm.

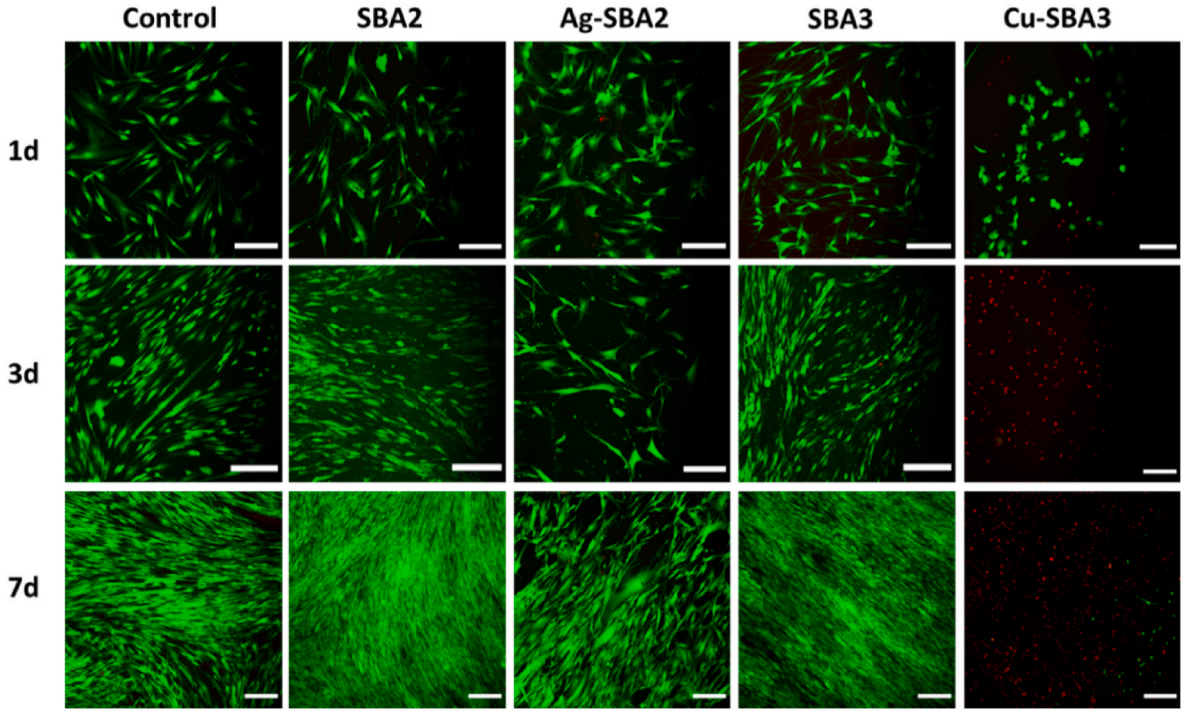

Fig. 9. Cell viability on fibronectin-coated bioactive glass discs at 1, 3, and 7d. Viability was analyzed with Live/dead staining. Scale bars 200 μm.

cultures are displayed in Fig. 11.

When comparing the release kinetics of Ag- and Cu-ions of the cell culture experiments with and without fibronectin (Fig. 9), in both cases the doped ions are seen to be released. However, some differences between the bare samples and the ones with adsorbed fibronectin were detected. In general, release kinetics follow the same pattern in both cases, where the ion leaching is most evident in the beginning of soaking in cell culture. In the case of Ag-SBA2, the release of Ag-ions continues until 7 days of cell culture, especially with the added fibronectin, where measured maximum Ag-ion concentration is seen to be higher. With the high standard deviations especially in the case of the 1-day timepoint, these differences could be simply due to the differences in the ion-exchange process. Regarding Cu-SBA3, the concentration of released Cu-ions was slightly lower with the presence of adsorbed fibronectin, but in both cases the Cu-ion release continues only until 3 days of soaking in the cell culture.

In addition, when comparing the Ag- and Cu-release of Fig. 11 to the one displayed in Fig. 6 with similar cell culture conditions, the overall release kinetics are found to follow a similar pattern. For Ag-SBA2 the release is seen to continue for 7 days in all measured conditions, also when soaked in pure α-MEM culture medium without added serum or cells (Fig. 3). However, in the case of Cu-SBA3, all the ICP measurements performed in cell culture conditions show Cu-ion release during 3 days of soaking (Figs. 6 and 11), while the Cu-ion release without added serum or cells (Fig. 3) occurs only until 1 day of soaking. It seems that the presence of cells delays the release of ion-exchanged Cu-ions from the Cu-SBA3 surface. In general, some differences in the maximum released concentrations of both Ag- and Cu-ions are detected between the different measurements, possibly due to inconsistencies in the ion exchange process. Especially in the case of Cu-SBA3 the differences in maximum release are found to be more evident, suggesting that the ion-exchange process of Cu-ions may lead to less uniform ion coating compared to Ag-doped SBA2.

Another way to prevent the negative effect of the initial ion release burst on the cells, glass discs were pre-incubated in the basic α-MEM culturing medium before cell culture. Especially in the *in vitro* static cell cultures, pre-treatment of BAG samples is recommended due to their high initial reactivity [44]. When BAGs get in contact with an aqueous environment, the fast ion-exchange phenomenon on their surface leads to a burst release of alkaline ions, and the following local pH increase [44,45]. The alkalinization of the surrounding medium to some extent is known to benefit alkaline phosphatase (ALP) activity and osteogenesis [46], but too high pH value, especially together with burst release of ions from the BAG can be detrimental to cell viability.

3.2.3. *Effect of glasses pre-incubation prior cell culture on hASCs*

The assessment of cell viability, proliferation, and morphology was carried out after pre-incubating glass discs for 24 h in a basic α-MEM culture medium before cell seeding. As displayed in Fig. 12, in the case of all the tested glasses, hASCs stayed viable in direct contact with glass

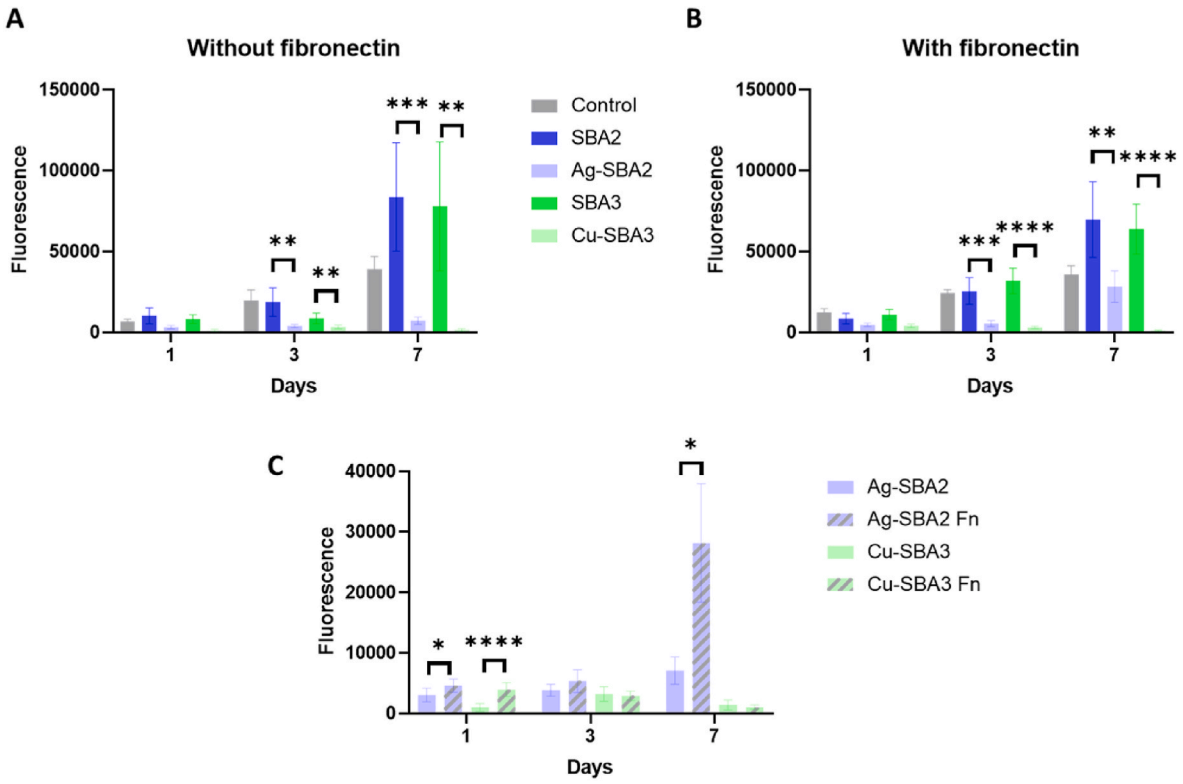

Fig. 10. Proliferation of hASCs cultured on TCPS (control), SBA2, Ag-SBA2, SBA3, and Cu-SBA3 discs for 7 days, A) without, or B) with fibronectin (Fn) coating, analyzed by CyQUANT Cell Proliferation Assay kit. C) Comparison of Ag-SBA2 and Cu-SBA3 with and without fibronectin (Fn) (*p < 0.05, **p < 0.01, ***p < 0.001, ****p < 0.0001).

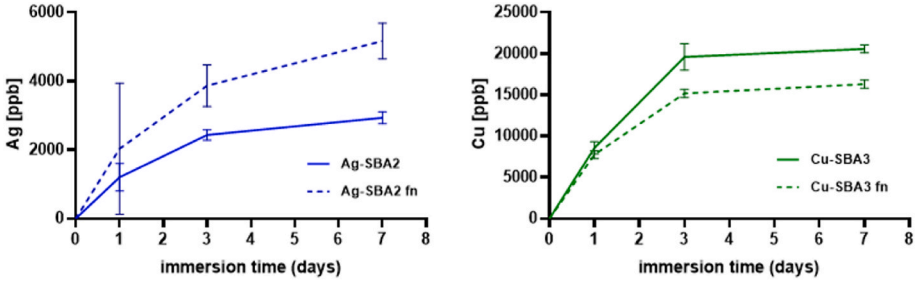

Fig. 11. Release of Ag and Cu ions from uncoated Ag-SBA2 and Cu-SBA3, compared to fibronectin (fn) -coated samples (Ag-SBA2-fn and Cu-SBA3-fn) measured by ICP-OES.

surfaces for up to 14 days. When comparing the undoped and Ag-/Cu -ion doped glasses, no difference in hASCs viability was detected. It seems that the 24 h pre-incubation is enough to limit the excessive surface reactivity of the studied BAGs.

In addition to the Live/Dead images, the cell proliferation during the 14 days of culture was assessed with CyQuant proliferation assay (Fig. 13). As demonstrated in Fig. 13, the cell proliferation followed a similar trend for all the compositions. Initially, during the first three days of culture, proliferation decreased for all compositions compared to the control, and the cell number is significantly lower on the doped glasses compared to the undoped ones. But after 14 days, the cell amount was approximately similar for all glasses and the control.

The ability of the hASCs to spread on the 24-h pre-incubated BAG discs was evaluated by staining the actin cytoskeleton and the nuclei. As evidenced in Fig. 14, the cell spreading was not affected by the glasses. All the cells grew in tight contact with each other forming a confluent cell layer, except in the case of Ag-SBA2, where individual cells are more evident due to lower cell growth. However, when observing the cell shape, all cells appeared spindle-shaped, which is known to be typical for MSCs [47].

In addition, the release of surface-doped ions is evaluated (Table 2) by ICP-OES analysis to assess whether using the standard pre-incubation time for bioactive glasses will eliminate the ion-exchanged layer of ions on the samples needed for the antibacterial effect [44].

As displayed in Tables 2 and in the case of Ag-SBA2, Ag-ions are being released from the surface already during the pre-incubation, but only partially. The majority of Ag-ions are released after one day in cell culture, and as seen in Figs. 10–12, this concentration does not seem to compromise hASCs viability in direct cell culture. The antibacterial effect of Ag-SBA2 has been previously proved for samples without pre-incubation [27], and therefore, further antibacterial evaluations would be needed to confirm that the pre-incubation does not prevent this effect. In the case of Cu-SBA3, a great majority of surface-doped Cu ions are released during the 24-h pre-incubation. Therefore, in the following cell culture, Cu-SBA3 resembles more its reference glass SBA3 without the ion-exchanged layer of Cu ions. It is also probable that the

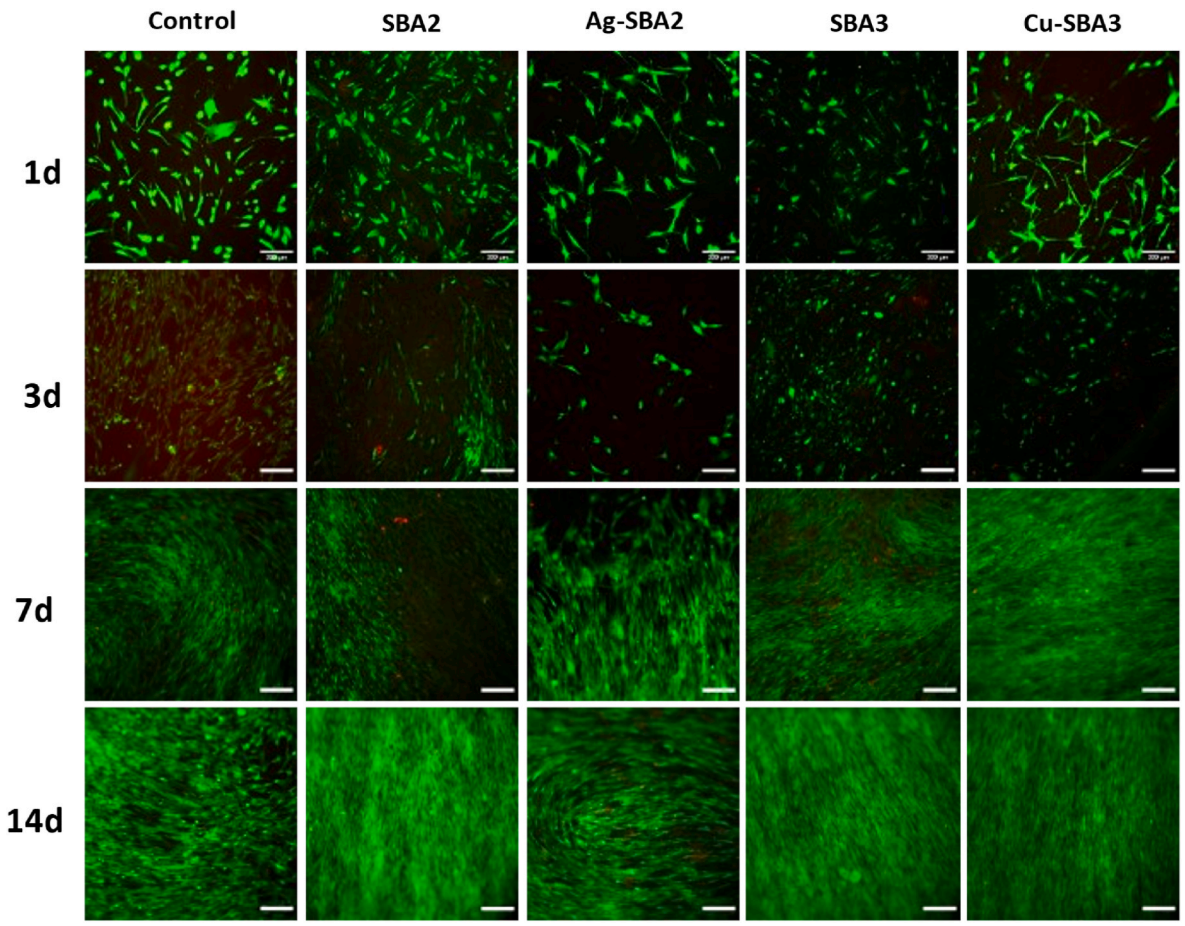

Fig. 12. Cell viability on pre-incubated bioactive glass discs at 1, 3, 7, and 14 days. Viability was analyzed with Live/dead staining. Scale bars 200 μm.

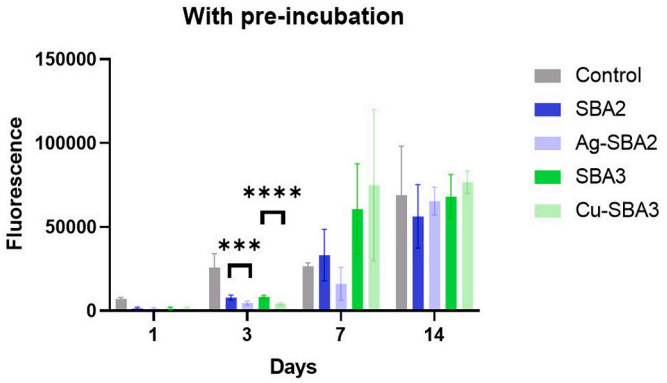

Fig. 13. Proliferation of hASCs cultured on TCPS (control), and on pre-incubated SBA2, Ag-SBA2, SBA3, and Cu-SBA3 discs for 14 days, analyzed by CyQUANT Cell Proliferation Assay kit (***$p < 0.001$, ****$p < 0.0001$).

possible antibacterial effect of Cu-SBA3 will be lost if pre-conditioning is used prior contact with the biological environment.

Balancing between the critical concentration for antibacterial performance and cytocompatibility is a challenge when optimizing multifunctional biomaterials for biomedical use. Above certain concentrations, both Ag^{+} and Cu^{2+} are known to be toxic to cells. However, it is difficult to state an exact toxic concentration due to the static *in vitro* culture conditions, where the lack of fluid flow and replenishment magnifies local concentrations and pH value changes. Therefore, instead of using preconditioning, which might compromise the release of antibacterial ions, the use of more dynamic culturing conditions could diminish the problem and prevent steep local ion concentration gradients toxic to cells [48,49]. It is also to be noted that rapid initial release of antibacterial ions, such silver or copper ions, could be necessary to treat early infection, even if it would also cause initial cell toxicity. In *vivo* conditions, new cells will be available, and once the first antimicrobial effect is implemented through burst release of antibacterial ions, the material surfaces are no longer found toxic and enable further cell adhesion and proliferation.

4. Conclusion

In this work, two bioactive glass compositions, SBA2 and SBA3, were prepared and studied both undoped and doped with antibacterial ionic silver (Ag-SBA2) and copper (Cu-SBA3) via ion-exchange process in aqueous solution to evaluate their cytocompatibility towards hASCs. The Live/Dead viability staining and CyQuant proliferation assay demonstrated the compromised hASCs viability with direct contact with both doped glasses. However, as evidenced by indirect culture with glass dissolution products, the cytotoxicity effect does not seem to arise from the dissolution products or specific ion concentrations in the medium, but rather from burst release and contact toxicity with the doped glass surfaces. The adsorption of fibronectin to glass surfaces improved the viability and proliferation of hASCs in contact with Ag-SBA2 but did not enhance the cytocompatibility of Cu-SBA3. In addition, the use of 24 h sample pre-incubation renders all samples cytocompatible, however with the possible loss of antibacterial Ag- or Cu-ions. As detected in EDS- and ICP analyses, the release of the Cu-ion layer from the surface of Cu-SBA3 occurs very abruptly during the first 24 h, which could further explain the compromised cytocompatibility compared to the more gradual and controlled release of Ag-ions from the surface of Ag-SBA2.

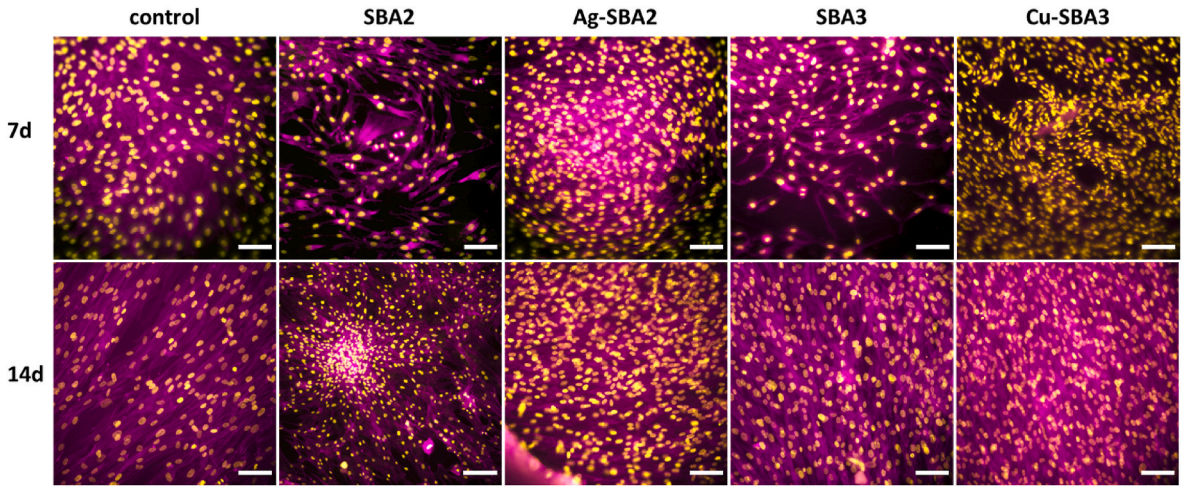

Fig. 14. Morphology of hASCs on TCPS (control), SBA2, Ag-SBA2, SBA3, and Cu-SBA3 discs in α-MEM complete medium analyzed by Nuclei (DAPI - yellow) and Actin (Phalloidin - magenta) immunostaining after 7 days and 14 days of culture. Scale bar 50 μm. (For interpretation of the references to color in this figure legend, the reader is referred to the Web version of this article.)

Table 2
Ag- and Cu-ion release, from Ag-SBA2 and Cu-SBA3, during pre-incubation and in between cell culture time points (0-1d, 1d-3d, 3d-7d), measured by ICP-OES. *) UDL = under the detection limit of the instrument.

Immersion interval	Ag-ion release [ppb] from Ag-SBA2	Cu-ion release [ppb] from Cu-SBA3
Pre-incubation 24 h	300.0 ± 141.4	21 433 ± 4921
In contact with hASCs 0-1d	5500 ± 707	150.0 ± 70.7
In contact with hASCs 1-3d	566.7 ± 152.8	UDL*
In contact with hASCs 3-7d	UDL*	UDL*

To utilize Cu-SBA3 for biomedical applications, further optimization of the ion-exchange process should be performed to ensure cell survival in contact with the glass surface. The results obtained in this study suggest the suitability of Ag-doped SBA2 to prevent early infection with its rapid release of Ag-ions and cytocompatibility. However, further data regarding stem cell differentiation ability and the antibacterial performance are needed in the future to confirm the suitability of Ag-SBA2 for use in bone infection treatment.

Author contributions

Conceptualization, M.L., A.H., M.M., J.M, and E.V.; formal analysis, M.L. and A.H.; investigation, M.L., A.H., M.M., J.M., E.V.; resources, S. M., J.M., and E.V.; writing – original draft preparation, M.L. and A.H.; writing – review and editing, M.L., A.H., M.M., S.M., J.M., and E.V.; supervision, J.M. and E.V.; project administration, M.M., J.M., and E.V.; funding acquisition, J.M. and E.V. All authors have read and agreed to the published version of the manuscript.

Declaration of competing interest

The authors declare that they have no known competing financial interests or personal relationships that could have appeared to influence the work reported in this paper.

Acknowledgments

The authors are funded under EXCELLENT SCIENCE - Marie Skłodowska-Curie Actions - Fostering new skills by means of excellent initial training of researchers, PREMUROSA, Grant agreement ID: 860462, https://cordis.europa.eu/project/id/860462.

This work made use of Tampere Microscopy Center facilities at Tampere University.

The authors acknowledge the Biocenter Finland (BF) and Tampere Imaging Facility (TIF) for the service.

Appendix A. Supplementary data

Supplementary data related to this article can be found at https://doi.org/10.1016/j.ceramint.2023.08.284.

References

[1] C.R.M. Black, V. Goriainov, D. Gibbs, J. Kanczler, R.S. Tare, R.O.C. Oreffo, Bone tissue engineering, Curr Mol Biol Rep 1 (3) (2015 Sep 1) 132–140.
[2] V.M. Schatkoski, T. Larissa do Amaral Montanheiro, B.R. Canuto de Menezes, R. M. Pereira, K.F. Rodrigues, R.G. Ribas, et al., Current advances concerning the most cited metal ions doped bioceramics and silicate-based bioactive glasses for bone tissue engineering, Ceram. Int. 47 (3) (2021) 2999–3012, helmikuu.
[3] B. Li, T.J. Webster, Bacteria antibiotic resistance: new challenges and opportunities for implant-associated orthopedic infections, J. Orthop. Res. 36 (1) (2018) 22–32.
[4] World Health Organization, Antimicrobial resistance: global report on surveillance [Internet] [cited 2022 Jan 23]. xxii, 232 pp. Available from:, World Health Organization, 2014 https://apps.who.int/iris/handle/10665/112642.
[5] N. Maffulli, R. Papalia, B. Zampogna, G. Torre, E. Albo, V. Denaro, The management of osteomyelitis in the adult, Surgeon 14 (6) (2016) 345–360, joulukuu.
[6] J.M. Sadowska, K.J. Genoud, D.J. Kelly, F.J. O'Brien, Bone biomaterials for overcoming antimicrobial resistance: advances in non-antibiotic antimicrobial approaches for regeneration of infected osseous tissue, Mater. Today 46 (2021) 136–154, kesäkuu.
[7] J.A. Wright, S.P. Nair, Interaction of staphylococci with bone, Int J Med Microbiol 300 (2) (2010) 193–204, helmikuu.
[8] L.L. Hench, An Introduction to Bioceramics, World Scientific, 1993, 406 pp.
[9] J.R. Jones, Review of bioactive glass: from Hench to hybrids, Acta Biomater. 9 (1) (2013) 4457–4486, tammikuu.
[10] Borkow G, Gabbay J. Copper as a biocidal tool. Curr. Med. Chem.. 12(18): 2163–2175.
[11] G. Franci, A. Falanga, S. Galdiero, L. Palomba, M. Rai, G. Morelli, et al., Silver nanoparticles as potential antibacterial agents, Molecules 20 (5) (2015 May) 8856–8874.
[12] B. Sugarman, Zinc and infection, Rev. Infect. Dis. 5 (1) (1983) 137–147, tammikuu.

[13] Z. Xu, X. Zhao, X. Chen, Z. Chen, Z. Xia, Antimicrobial effect of gallium nitrate against bacteria encountered in burn wound infections, RSC Adv. 7 (82) (2017 Nov 7) 52266–52273.
[14] O.L. Pop, A. Mesaros, D.C. Vodnar, R. Suharoschi, F. Tăbăran, L. Mageruşan, et al., Cerium oxide nanoparticles and their efficient antibacterial application in vitro against gram-positive and gram-negative pathogens, Nanomaterials 10 (8) (2020 Aug) 1614.
[15] J.L. Clement, P.S. Jarrett, Antibacterial silver, Met-Based Drugs. 1 (5–6) (1994) 467–482.
[16] X. Wang, S. Liu, M. Li, P. Yu, X. Chu, L. Li, et al., The synergistic antibacterial activity and mechanism of multicomponent metal ions-containing aqueous solutions against Staphylococcus aureus, J. Inorg. Biochem. 163 (2016) 214–220, lokakuu.
[17] M. Diba, A.R. Boccaccini, 9 - silver-containing bioactive glasses for tissue engineering applications, in: N. Baltzer, T. Copponnex (Eds.), Precious Metals for Biomedical Applications [Internet], Woodhead Publishing, 2014 [cited 2022 Jan 21]. pp. 177–211. Available from: https://www.sciencedirect.com/science/article/pii/B9780857094346500093.
[18] H. Xie, P. Wang, J. Wu, Effect of exposure of osteoblast-like cells to low-dose silver nanoparticles: uptake, retention and osteogenic activity, Artif. Cells, Nanomed. Biotechnol. 47 (1) (2019) 260–267, joulukuu.
[19] S. Kargozar, M. Mozafari, S. Ghodrat, E. Fiume, F. Baino, Copper-containing bioactive glasses and glass-ceramics: from tissue regeneration to cancer therapeutic strategies, Mater. Sci. Eng. C 121 (2021), 111741 helmikuu.
[20] J. Rivadeneira, A. Gorustovich, Bioactive glasses as delivery systems for antimicrobial agents, J. Appl. Microbiol. 122 (6) (2017) 1424–1437.
[21] H. Palza, B. Escobar, J. Bejarano, D. Bravo, M. Diaz-Dosque, J. Perez, Designing antimicrobial bioactive glass materials with embedded metal ions synthesized by the sol–gel method, Mater. Sci. Eng. C 33 (7) (2013) 3795–3801, lokakuu.
[22] Y.F. Goh, A.Z. Alshemary, M. Akram, M.R. Abdul Kadir, R. Hussain, Bioactive glass: an in-vitro comparative study of doping with nanoscale copper and silver particles, Int. J. Appl. Glass Sci. 5 (3) (2014) 255–266.
[23] L.C.A. da Silva, F.G. Neto, S.S.C. Pimentel, R. da S. Palácios, F. Sato, K.M. Retamiro, et al., The role of Ag2O on antibacterial and bioactive properties of borate glasses, J. Non-Cryst. Solids 554 (2021), 120611 helmikuu.
[24] M. Miola, G. Fucale, G. Maina, E. Verné, Antibacterial and bioactive composite bone cements containing surface silver-doped glass particles, Biomed. Mater. 10 (5) (2015 Oct), 055014.
[25] M. Miola, E. Verné, Bioactive and antibacterial glass powders doped with copper by ion-exchange in aqueous solutions, Materials 9 (6) (2016 Jun) 405.
[26] M. Miola, A. Cochis, A. Kumar, C.R. Arciola, L. Rimondini, E. Verné, Copper-doped bioactive glass as filler for PMMA-based bone cements: morphological, mechanical, reactivity, and preliminary antibacterial characterization, Materials 11 (6) (2018 Jun) 961.
[27] A. Cochis, J. Barberi, S. Ferraris, M. Miola, L. Rimondini, E. Vernè, et al., Competitive surface colonization of antibacterial and bioactive materials doped with strontium and/or silver ions, Nanomaterials 10 (1) (2020 Jan) 120.
[28] L. Kyllönen, S. Haimi, B. Mannerström, H. Huhtala, K.M. Rajala, H. Skottman, et al., Effects of different serum conditions on osteogenic differentiation of human adipose stem cells in vitro, Stem Cell Res. Ther. 4 (1) (2013 Feb 15) 17.
[29] M. Patrikoski, M. Juntunen, S. Boucher, A. Campbell, M.C. Vemuri, B. Mannerström, et al., Development of fully defined xeno-free culture system for the preparation and propagation of cell therapy-compliant human adipose stem cells, Stem Cell Res. Ther. 4 (2) (2013 Mar 7) 27.
[30] L. Hyväri, M. Ojansivu, M. Juntunen, K. Kartasalo, S. Miettinen, S. Vanhatupa, Focal adhesion kinase and ROCK signaling are switch-like regulators of human adipose stem cell differentiation towards osteogenic and adipogenic lineages, Stem Cell. Int. (2018), 2190657, 2018 Sep. 12.
[31] M. Dominici, K. Le Blanc, I. Mueller, I. Slaper-Cortenbach, F. Marini, D. Krause, et al., Minimal criteria for defining multipotent mesenchymal stromal cells. The International Society for Cellular Therapy position statement, Cytotherapy 8 (4) (2006) 315–317.
[32] P. Bourin, B.A. Bunnell, L. Casteilla, M. Dominici, A.J. Katz, K.L. March, et al., Stromal cells from the adipose tissue-derived stromal vascular fraction and culture expanded adipose tissue-derived stromal/stem cells: a joint statement of the International Federation for Adipose Therapeutics and Science (IFATS) and the International Society for Cellular Therapy (ISCT), Cytotherapy 15 (6) (2013 Jun) 641–648.
[33] H. Li, K.W. Michael Siu, R. Guevremont, J.C. Yves Le Blanc, Complexes of silver(I) with peptides and proteins as produced in electrospray mass spectrometry, J. Am. Soc. Mass Spectrom. 8 (8) (1997 Aug 1) 781–792.
[34] D. Titus, E. James Jebaseelan Samuel, S.M. Roopan, Chapter 12 - nanoparticle characterization techniques, in: A.K. Shukla, S. Iravani (Eds.), Green Synthesis, Characterization and Applications of Nanoparticles [Internet], Elsevier, 2019 [cited 2022 Jul 19]. pp. 303–19. (Micro and Nano Technologies). Available from: https://www.sciencedirect.com/science/article/pii/B9780081025796000125.
[35] F. Markoulidis, A Review on Surface Analysis Techniques, 2009.
[36] S. Cai, C. Wu, W. Yang, W. Liang, H. Yu, L. Liu, Recent advance in surface modification for regulating cell adhesion and behaviors, Nanotechnol. Rev. 9 (1) (2020 Jan 1) 971–989.
[37] N.J. Thyparambil, L.C. Gutgesell, C.C. Hurley, L.E. Flowers, D.E. Day, J.A. Semon, Adult stem cell response to doped bioactive borate glass, J. Mater. Sci. Mater. Med. 31 (2) (2020 Jan 21) 13.
[38] A. Mishra, M. Ojansivu, R. Autio, S. Vanhatupa, S. Miettinen, J. Massera, In-vitro dissolution characteristics and human adipose stem cell response to novel borophosphate glasses, J. Biomed. Mater. Res. 107 (9) (2019) 2099–2114.
[39] B. Cao, Y. Zheng, T. Xi, C. Zhang, W. Song, K. Burugapalli, et al., Concentration-dependent cytotoxicity of copper ions on mouse fibroblasts in vitro: effects of copper ion release from TCu380A vs TCu220C intra-uterine devices, Biomed. Microdevices 14 (4) (2012 Aug 1) 709–720.
[40] M.P. Cervantes-Cervantes, J.V. Calderón-Salinas, A. Albores, J.L. Muñoz-Sánchez, Copper increases the damage to DNA and proteins caused by reactive oxygen species, Biol. Trace Elem. Res. 103 (3) (2005 Mar 1) 229–248.
[41] M. Miola, E. Bertone, E. Vernè, In situ chemical and physical reduction of copper on bioactive glass surface, Appl. Surf. Sci. 495 (2019 Mar 30), 143559.
[42] L. Parisi, A. Toffoli, B. Ghezzi, B. Mozzoni, S. Lumetti, G.M. Macaluso, A glance on the role of fibronectin in controlling cell response at biomaterial interface, Jpn Dent Sci Rev 56 (1) (2020 Mar 1) 50–55.
[43] L. Azizi, P. Turkki, N. Huynh, J.M. Massera, V.P. Hytönen, Surface modification of bioactive glass promotes cell attachment and spreading, ACS Omega 6 (35) (2021 Sep 7) 22635–22642.
[44] F.E. Ciraldo, E. Boccardi, V. Melli, F. Westhauser, A.R. Boccaccini, Tackling bioactive glass excessive in vitro bioreactivity: preconditioning approaches for cell culture tests, Acta Biomater. 75 (2018) 3–10, heinäkuu.
[45] A. Li, Y. Lv, H. Ren, Y. Cui, C. Wang, R.A. Martin, et al., In vitro evaluation of a novel pH neutral calcium phosphosilicate bioactive glass that does not require preconditioning prior to use, Int. J. Appl. Glass Sci. 8 (4) (2017) 403–411.
[46] J. Tan, D. Wang, H. Cao, Y. Qiao, H. Zhu, X. Liu, Effect of local alkaline microenvironment on the behaviors of bacteria and osteogenic cells, ACS Appl. Mater. Interfaces 10 (49) (2018 Dec 12) 42018–42029.
[47] T. Debnath, L.K. Chelluri, Standardization and quality assessment for clinical grade mesenchymal stem cells from human adipose tissue, Hematol Transfus Cell Ther 41 (1) (2019) 7–16.
[48] L. Hupa, S. Fagerlund, J. Massera, L. Björkvik, Dissolution behavior of the bioactive glass S53P4 when sodium is replaced by potassium, and calcium with magnesium or strontium, J. Non-Cryst. Solids 432 (2016 Jan 15) 41–46.
[49] S. Taipale, P. Ek, M. Hupa, L. Hupa, Continuous measurement of the dissolution rate of ions from glasses, Adv. Mater. Res. 39–40 (2008) 341–346.